The International Journal of Cardiovascular Imaging (2019) 35:367–374
https://doi.org/10.1007/s10554-019-01539-3

ORIGINAL PAPER

Image quality and radiation dose of ECG-triggered High-Pitch Dual-Source cardiac computed tomography angiography in children for the evaluation of central vascular stents

Christian A. Barrera[1] · Hansel J. Otero[1] · Ammie M. White[1] · David Saul[1] · David M. Biko[1]

Received: 9 May 2018 / Accepted: 17 January 2019 / Published online: 25 January 2019

Abstract
Assess image quality and radiation dose of ECG-triggered High-Pitch Dual-Source CTA for the evaluation central vascular stents in children. We included all children ≤ 21 years old with one or more central vascular stents and available prospective ECG-triggered High-Pitch Dual-Source CTA performed at our institution between January 2015 and August 2017. Demographic and scanner information was retrieved. Two board-certified pediatric radiologists blinded to the clinical data, independently reviewed and scored each case using a four-point quality score. Scores 1, 2 and 3 were considered of diagnostic image quality. Inter-observer agreement and non-parametric test were used. 18 patients (10 girls, 8 boys) with a mean age of 9.47 ± 7.38 years (mean ± SD) met inclusion criteria. Thirty-two central vascular stents were evaluated. Mean quality score was 2.07 ± 0.94 with 12.5% (4/32) of the cases classified as unevaluable. Interobserver agreement was excellent (k = 0.86). There is no significant difference between quality score and stent location (p = 0.07). There is a significant difference with stent material as all non-diagnostic scores were only seen in covered stents made of platinum-iridium (p < 0.001). There was no association between image quality and age, height, weight, BSA, heart rate, radiation dose or stent lumen size (p > 0.05). ECG-triggered high-pitch spiral DS-CTA offers appropriate image quality for assessment of central vascular stents in children.

Keywords Children · Cardiac CT · Stent · Dual-source CT · High Pitch · ECG-triggered

Introduction

Congenital heart disease (CHD) is associated with other vascular anomalies such as stenosis of thoracic vessels [1, 2]. Stents are used to treat vascular stenosis in children, including hybrid approaches that may combine surgical and trans-catheter interventions [3–6]. Complications related to stent placement, like in-stent stenosis and aneurysm formation, require imaging follow-up [7]. Conventional invasive angiography is the gold standard in clinical practice for in-stent stenosis assessment and follow-up, as it allows direct visualization of the stent and treatment [8]. However, it is considered as invasive, expensive and limited in some medical centers [9]. Computed tomography angiography (CTA) is considered a practical alternative for assessment of central vascular stents in children and may be particularly helpful for stent evaluation or post-procedure complications [7, 10].

The increased use of CTA in clinical practice has raised concerns regarding risks related to radiation in children [11]. Children are more susceptible to ionizing radiation because they are constantly growing, their tissues have a higher cell division rate, and have longer life expectancy for oncogenic effects to develop [12]. The ALARA principle ("as low as reasonably achievable") looks to reduce radiation exposure in children through the improvement of imaging protocols, scanner techniques, and protection measures [13]. Newer technologies allows to maintain image quality while decreasing radiation exposure and acquisition times [14]. Cardiovascular imaging in particular requires fast acquisition because the constant cardiac motion impairs image quality. Initially, single-source scanners using high pitch values yield under-sampled data caused by acquisition gaps. Later on, dual-source systems were developed using two tubes and two corresponding detectors mounted into the gantry.

✉ Christian A. Barrera
barreracac@email.chop.edu

[1] Department of Radiology, Children's Hospital of Philadelphia, Philadelphia, PA, USA

The second tube allows gapless z-sampling at high-speed table depending on the field of view [15]. However, because both tubes are acquiring data over different anatomies, the potential advantages of dual energy techniques including spectral manipulation and virtual non-contrast studies are lost [16]. Second generation dual-source computed tomography (DSCT) scanners include a high-pitch spiral acquisition mode that further improves temporal resolution and promises to lower the radiation doses. This system, associated with a prospective ECG-triggered protocol, has been reported to produce high quality images in children with CHD undergoing cardiac imaging [17, 18]. However, because this technique uses lower radiation dose, low image quality and diagnostic performance remain valid concerns. To our knowledge, there are no studies assessing central vascular stents using this CTA technology. The purpose of this study is to determine the image quality and radiation dose of dual source with prospective ECG-triggered High-Pitch CTA for the assessment of central vascular stents in children.

Materials and methods

This is a retrospective study approved by our Institutional Review Board and performed in compliance with the Health Insurance Portability and Accountability Act. The need for written informed consent was waived in view of the retrospective nature of the research. We searched the imaging records at our institution from January 2015 through August 2017 for all patients between 0 and 21 years of age with one or more central vascular stents who underwent prospective ECG-triggered High-Pitch Dual-Source CTA of the chest. Demographics (e.g. age, gender, height, weight, indication for stent placement, indication for CTA, stent location), CT parameters (e.g. injection rate, radiation dose), and stent characteristics (e.g. covered, material) were retrieved from the electronic health record.

All studies were performed with a prospectively ECG-triggered High-Pitch, Dual-Source spiral acquisition scanner (Flash Spiral Cardio, Siemens Healthcare, Forchheim, Germany). CT parameters are as follows: $2 \times 128 \times 0.6$-mm slice collimation using a z-flying focal spot technique; 0.28 s gantry rotation time; pitch 3.0 and temporal resolution 75 ms. Automated tube voltage and current were used according to patient's size and anatomic region. Beta-blockers were not used in any of the patients. Sedation was used according to clinical condition and patients' age. Patients older than 6 years of age were asked to hold their breath during the image acquisition while younger children do not receive breathing instructions. A non-ionic, low-osmolar iodinated contrast agent (Iohexol, Omnipaque™, 350 mg/mL, GE Healthcare inc) was injected via a peripheral intravenous access at a 2 mL/kg dose (up to a maximum dose of 100 mL), followed by a bolus of normal saline at the same flow rate with the use of a dual-head power injector (Medrad Inc, Warrendale, United States). Injection rate was set considering the available intravenous access catheter and calculated to achieve an infusion duration between 10 and 20 s. An auto-triggered bolus tracking technique was used in all cases with a region of interest in the left ventricle, descending aorta or right ventricle based on the study's original clinical indication. Cardiac phase was selected automatically by the scanner according to the patient's heart rate (i.e. diastolic phase with heart rates ≤ 80 bpm, end systole phase for heart rates > 80 bpm). Image reconstruction was made using iterative reconstruction technique (Sinogram Affirmed Iterative Reconstruction (SAFIRE), Siemens Healthcare, Forchheim, Germany) which applies a noise-modeling technique based on the original raw data.

The volume CT dose index ($CTDI_{vol}$) and dose-length product (DLP) were systematically retrieved from each study, which is reported by our scanners and referenced to the 32-cm CTDI phantom. In order to calculate the effective dose (mSv), using DLP mSv conversion factors for chest as published in AAPM Report 96, an additional factor of 2 was multiplied for patients under the age of 14 [19].

Two board-certified pediatric radiologists with 8 years and 4 years of experience and special interest in cardiovascular imaging, who were blinded to the clinical data, independently reviewed each case. For subjective image quality assessment, we used a four-point scale: (1) excellent image quality, no artifact affecting evaluation of stent; (2) good quality, mild artifact or blurring of in-stent detail including heterogeneous appearance but acceptable for diagnosis; (3) acceptable quality, moderate artifact present but images still interpretable; (4) unevaluable, severe artifact renders interpretation not possible. Scores 1, 2 and 3 were considered of diagnostic image quality. The scale was agreed beforehand between the readers using clinical examples, as shown in Fig. 1, similar to previously published methodology [20, 21].

Statistical analysis was performed using SPSS version 23 (IBM, Armonk, NY) software. Continuous variables were presented as mean ± standard deviation and categorical variables as percentages and counts. Inter-observer agreement was evaluated with kappa statistics. Scores of 0.20 or less was considered slight agreement, 0.21–0.40 fair agreement, 0.41–0.60 moderate agreement, 0.61–0.80 substantial agreement and 0.81–0.99 as almost perfect agreement [22]. We used Kruskal–Wallis test to compare the four-point image quality scale against the continuous and categorical variables. A two-tailed p-value of < 0.05 was considered significant.

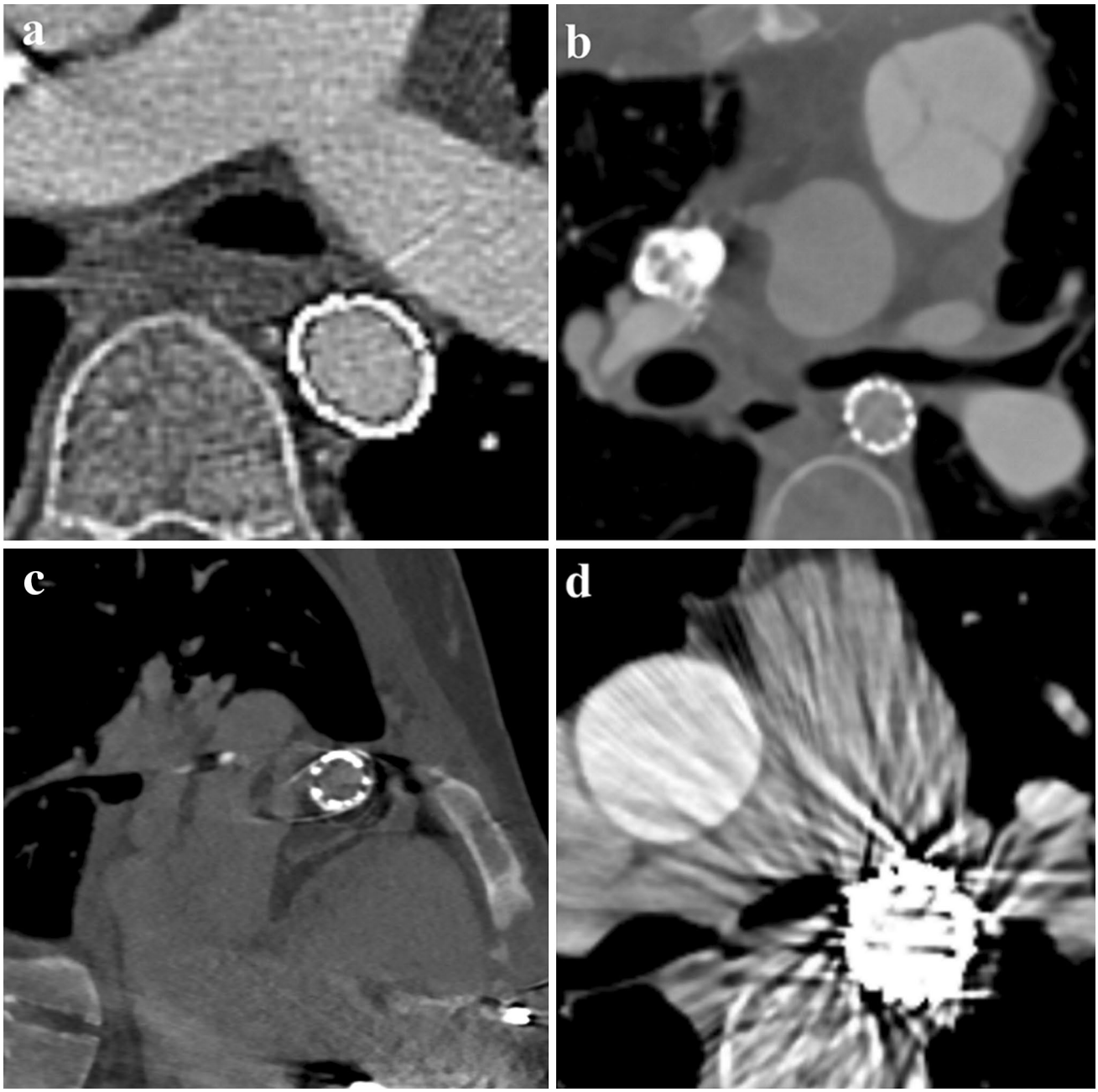

Fig. 1 Representative stent images that illustrates the four image quality scores. **a** 1—excellent image quality, no artifact affecting evaluation of stent (*axial view*); **b** 2—good quality, mild artifact or blurring of in-stent detail including heterogeneous appearance but acceptable for diagnosis (*axial view*); **c** 3—acceptable quality, moderate artifact present but images still interpretable (*sagittal oblique view of the stent short-axis using multi-planar reconstruction*); **d** 4—unevaluable, severe artifact renders interpretation not possible (*axial view*)

Results

A total of 18 patients (10 girls, 8 boys) with a mean age of 9.47 ± 7.38 years (range 0–21 years) and 32 individual stents met inclusion criteria. The mean age for boys and girls were 9.08 ± 5.48 years and 9.70 ± 8.45 years, respectively. Patients' anthropometric measurements and study indications are resume in Table 1. The mean CTDI, DLP and effective dose were 3.47 ± 2.01 mGy, 98.29 ± 66.02 mGy × cm and 2.08 ± 0.84 mSv, respectively, Table 2. Tube voltage used in our sample varied between 70 and 120 kVp according to patient size. The most common stent location was the descending aorta (9/32), followed by the left (5/32) and right pulmonary arteries (5/32). The stent materials seen on our population were stainless steel (n = 23), platinum/chromium (n = 4) and platinum/iridium

Table 1 Clinical information, indication, scan parameters and heart rate at the time of CT acquisition

Variable (N = 18)	Results (mean ± SD, range)
Age (years)	9.47 ± 7.38 (0–21)
Gender	Girls 10, Boys 8
Height (cm)	124.56 ± 43.79 (58.2–182.8)
Weight (kg)	37.25 ± 4.19 (5.4–100.0)
BMI (kg/m^2)	20.03 ± 4.19 (14.95–37.18)
BSA (m^2)	1.10 ± 0.60 (0.30–2.13)
Heart rate at exam (bpm)	93.23 ± 26.46 (47–127)
Radiation dose (mSv)	2.08 ± 0.84 (0.92–4.53)
CTDIvol (mGy)	3.47 ± 2.01 (0.93–7.27)
DLP (mGy cm)	98.29 ± 66.02 (17.6–204.9)
Stent diameter (mm)	12.07 ± 4.73 (5.1–22)
Diagnosis	
Coarctation of the aorta	6
Truncus arteriosus	3
Transposition of great arteries	3
Heterotaxy syndrome	2
Tetralogy of Fallot	2
Other	2

BMI body mass index, *BSA* body surface area, *CTDI* Computed Tomography Dose Index, *DLP* dose length product, *SD* standard deviation

(n = 4) and the most common stent brand was Genesis Palmaz (n = 18), Table 3. Unfortunately, one of the stents was implanted outside our institution and no size, material or brand information was available in our medical records. Three (16.6%) were under general anesthesia and four (22.2%) received moderate conscious sedation, which was decided in consultation with a nurse and anesthesiologist from our sedation unit, as per departmental protocol. There were no contrast adverse events nor complications during the study acquisition and all patients left the room in stable conditions after image acquisition.

The mean quality scores were 2.00 ± 1.04 for reader 1 and 2.16 ± 1.01 for reader 2. The mean quality score between both readers was 2.07 ± 0.94 with 12.5% (4/32) of the cases classified as unevaluable. Combining both readers' scores, 87.5% (28/32) were considered to have diagnostic image quality and 20% (6/30) had excellent quality. Inter-observer agreement was almost perfect ($k = 0.86$). There is no significant difference between quality score with stent location ($p = 0.07$, Table 4) and sedation ($p = 0.37$). However, there is a significant difference between image quality and stent material as all non-diagnostic scores were only seen in covered stents made of platinum-iridium ($p < 0.001$). This alloy's cover is composed of expanded polytetrafluoroethylene (ePTFE). There was no association between image quality and age, height, weight, BSA, heart rate, radiation dose, contrast dose, contrast infusion rate or stent lumen size ($p > 0.05$).

Discussion

Our results show that prospective ECG-triggered High-Pitch Dual-Source CTA renders diagnostic image quality and low radiation dose for assessment of central vascular stents in children. In total, 87% of stents evaluated in this study showed diagnostic image quality; while all studies of covered stents were deemed uninterpretable. Multiple technological advances have been made throughout the years to improve cardiovascular evaluation via computed tomography [14]. The advent of newer generation CT scanners, faster image acquisition and reconstruction algorithms have allowed better depiction of small stents in adults compared to the first reports published in 1995 [14]. Great vessel stent depiction on CT has not been studied as thoroughly as coronary stents. Two in-vitro studies investigated imaging with CT and MRI with great vessel stents. Nordmeyer et al. [23] compared MRI, CT and conventional angiography for assessment of great vessel stents in-vitro. They observed a comparable diagnostic accuracy between conventional angiography and CT; however, streak artifacts and thickening of metallic struts are related to CT imaging and stent material. Den Harder et al. [24] also compared large vessel stents on MRI and 256-slice multidetector computed tomography (MDCT) in-vitro reporting an 88% stent lumen visibility rate using CT. It seems that CT yields better great vessel stent depiction compared to MRI at the expense of slightly underestimating stent diameter [23, 24]. Eichhorn et al. [10]

Table 2 Effective dose and body mass index according to age groups

Age group	BSA	CTDI	DLP	Effective dose
0–5 years (n = 12)	0.46 ± 0.17	1.48 ± 0.48	29.10 ± 11.51	1.57 ± 0.58
5–10 years (n = 5)	0.99 ± 0.11	2.96 ± 1.34	84.16 ± 36.69	2.91 ± 1.48
10–15 years (n = 5)	1.84 ± 0.12	5.51 ± 0.54	172.38 ± 35.52	2.41 ± 0.48
> 15 years (n = 10)	1.58 ± 0.29	5.09 ± 1.43	151.33 ± 30.88	2.11 ± 0.43
Total (n = 32)	1.10 ± 0.60	3.47 ± 2.00	98.29 ± 66.02	2.08 ± 0.84

BMI body mass index, *BSA* body surface area, *CTDI* Computed Tomography Dose Index, *DLP* dose length product

Table 3 Overview of stent characteristics and location

Variable (N = 32)	Results
Stent material and brand	
Stainless steel (n = 23)	
Genesis Palmaz	18
Intrastent Mega LD	3
Intrastent Max LD	2
Platinum/chromium	
Rebel platinum	4
Platinum/iridium	
Mounted CP Stent NuMED	4
Unavailable information	1
Cover	
Covered stents	4
Uncovered stents	27
Unavailable information	1
Location (diagnosis)	
Descending Aorta	9 (7 Coarctation of aorta, 4 TA)
Right Pulmonary Artery	5 (2 TOF, 2 TA, 2 TGA)
Left Pulmonary Artery	5 (1 TOF, 2 TA, 2 TGA)
Ascending Aorta	3 (3 Coarctation of aorta)
Main Pulmonary Artery	3 (1 Heterotaxy syndrome, 1 TA, 1 TGA)
Inferior Vena Cava	2 (2 Heterotaxy syndrome)
Other	5

TOF Tetralogy of Fallot, *TA* Truncus arteriosus, *TGA* transposition of the greater arteries

Table 4 Quality score divided by reader according to the stent location

Location	Mean ± SD		
	Reader 1	Reader 2	Final score
Descending aorta (n = 9)	2.33 ± 1.32	2.11 ± 1.45	2.22 ± 1.37
Right Pulmonary Artery (n = 5)	1.60 ± 0.89	2.00 ± 0.70	1.80 ± 0.75
Left Pulmonary Artery (n = 5)	1.20 ± 0.44	1.60 ± 0.89	1.40 ± 0.41
Ascending aorta (n = 3)	2.33 ± 0.57	1.67 ± 0.57	2.00 ± 0.01
Main Pulmonary Artery (n = 3)	2.67 ± 0.57	2.67 ± 0.57	2.67 ± 0.57
Inferior Vena Cava (n = 2)	1.50 ± 0.70	2.00 ± 0.01	1.75 ± 0.35
Other (n = 5)	2.20 ± 1.30	3.00 ± 0.70	2.60 ± 0.89

SD standard deviation

showed in-vivo good agreement between conventional angiography and MDCT imaging (pitch values between 1.25 and 0.31) with higher radiation exposure not related to higher image quality. High-Pitch Dual-Source CTA in particular has shown promising results for stent depiction in children and adults using either retrospective or prospective scanning protocols [17, 25–27]. Both retrospective and prospective protocols are similar in terms of image quality; however, radiation dose delivered by retrospective gating is higher and should be avoided in children [28, 29]. Prospective protocols achieve diagnostic image quality while delivering a lower radiation dose. Recent studies have proposed further analysis of fluid dynamics during the post processing of cross sectional imaging studies. Computational fluid dynamics provide hemodynamic information such as pressure gradients [30, 31], which could prove useful in the assessment of patients with coarctation of the aorta before and after stent placement. However, the use of intravenous contrast and increment of radiation may lead to use MRI instead of CT for this purpose [32, 33]. However, additional studies are needed to validate the utility of these models in children.

Age, heart rate, and anthropometric measurements are factors related to image quality that contribute to adequate coronary arteries depiction on ECG-triggered CTA [18, 26, 34]. For example, the evaluation of very small coronary arteries in younger children is limited by CT's inherent spatial resolution [35]. It is also known that stents smaller than 3 mm in diameter can impair image quality considerably on CT [28, 36–38]. However, none of the stents assessed in the present study had a diameter < 3 mm with the smallest measuring 5 mm. This might explain why we did not find a significant difference between stent location and diameter with image quality. Similarly, high heart rates shorten the cardiac rest period, impairing image quality on ECG-triggered CTA and overcoming the scanner's temporal resolution [39]. Nonetheless, it seems that none of these factors played an important role for central vascular stent depiction on CTA.

Stent characteristics must be considered when choosing which imaging modality to use for follow-up. Stent material is an important factor that may influence image quality. The ideal stent material should have good expandability, flexibility, sufficient radial hoop, adequate radiopacity, and be resistant to thrombosis [40]. For these reasons, metallic stents are most frequently preferred and multiple alloys are available to choose from in the market. These alloys have shown to have excellent biocompatibility, adequate mechanical behavior and high radiopacity [40–42]. All covered stents made of platinum-iridium in our sample (n = 4) yielded uninterpretable image quality, Fig. 1d. Nordmeyer et al. [23] and Den Harder et al. [24] observed significant metallic streak artifacts in CT images with platinum-iridium covered stents. While a previous study shows that the cover material does not play a role on imaging artifacts [43]. MRI showed to be an alternative option to depict these stents using high flip angle with a gradient recall echo sequence, steady-state free precession sequence or high flip angle MR angiography [23]. However, MRI tends to underestimate diameter in non-stenosed stents and overestimates diameter in internally stenosed stents [23]. This may lead to use MRI for follow-up

in patients with platinum-iridium stents and CT for those with stainless steel or platinum-chromium stents.

The average effective radiation dose observed in our sample (2.07 mSv) was considerably higher with respect to studies evaluating infants [25–27]. However, 62% of our sample was older than 5 years old, with higher effective doses (Table 2). Additionally, other authors have reported using higher pitch values (between 3.2 and 3.4), resulting in effective doses between 0.40 and 1.30 mSv [17, 25–27]; while we use a pitch of 3.0. Also important is that in our current sample, all chest CTAs included the entire chest, including both lungs; while in other practices cardiac CTAs z-axis coverage is limited to the heart. This difference in z-axis coverage is likely a major determinant of differences in dose. Moreover, other authors using comparable protocols obtained similar effective doses as ours. Lell et al. and Kim et al. reported using prospectively ECG-triggered Dual-Source CTA (with a pitch of 3.0) an average effective doses of 1.90 and 1.82 mSv, respectively [44, 45]. Further measurements could be used to improve our protocols, phantoms using a pitch value 3.2 has shown to reduce doses up to 52% with excellent image quality [46]. It is difficult to speculate if using a 3.4 pitch value would maintain image quality at expenses of reducing radiation dose. However, assessment of coronary stents in adults and coronary arteries in children using dual-source CTA with a pitch value of 3.4 have yield excellent image quality [17, 47]. Considering coronary stents are smaller than central vascular stents, it would be safe to assume that increasing the pitch value would not significantly affect image quality. However, more studies are need it to confirm this statement.

Our study has several limitations. First, it is a retrospective descriptive study performed at a single pediatric institution. Second, the relatively small number of stents assessed (n = 32) limited the number of clinical conditions and stent types in our sample. Third, we did not have complete stenosis cases and thus we could not calculate a minimum lumen obstruction cut-off for in-stent stenosis on CTA. Finally, the lack of stent information and digital angiography for correlation and confirmation has to be considered for interpretation of these results. While CT has proven to be an excellent imaging technique for stent depiction, digital angiography remains the gold standard for stent evaluation and diagnosis of in-stent stenosis. Because some procedures were performed on our study cohort at other institutions, their medical records have missing information.

Conclusion

Prospective ECG-triggered High-Pitch Dual-Source spiral acquisition cardiac computed tomography angiography provides consistent and appropriate image quality for evaluation of central vascular stents in children. Moreover, good diagnostic image quality is attainable in all patients and not affected by age, anthropometric measurements, or heart rate. Additional studies might focus in identifying appropriate imaging for those patients with platinum-iridium stents.

Compliance with ethical standards

Conflict of interest The authors declare that they have no conflicts of interest.

Informed consent The need for written informed consent was waived in view of the retrospective nature of the research.

Statement of human rights All procedures followed were in accordance with the ethical standards of the responsible committee on human experimentation (institutional and national) and with the Declaration of Helsinki of 1964, as revised in 2008

References

1. Meot M, Lefort B, El Arid JM, Soule N, Lothion-Boulanger J, Lengelle F, Chantepie A, Neville P (2017) Intraoperative stenting of pulmonary artery stenosis in children with congenital heart disease. Ann Thorac Surg 104(1):190–196. https://doi.org/10.1016/j.athoracsur.2016.12.012
2. Temel MT, Coskun ME, Baspinar O, Demiryurek AT (2017) Prevalence and characteristics of coronary artery anomalies in children with congenital heart disease diagnosed with coronary angiography. Turk Kardiyoloji Dernegi arsivi: Turk Kardiyoloji Derneginin yayin organidir 45(6):527–532. https://doi.org/10.5543/tkda.2017.24162
3. Lynch W, Boekholdt SM, Hazekamp MG, de Winter RJ, Koolbergen DR (2015) Hybrid branch pulmonary artery stent placement in adults with congenital heart disease. Interact Cardiovasc Thorac Surg 20(4):499–503. https://doi.org/10.1093/icvts/ivu435
4. Agrawal H, Alkashkari W, Kenny D (2017) Evolution of hybrid interventions for congenital heart disease. Expert Rev Cardiovasc Ther 15(4):257–266. https://doi.org/10.1080/14779072.2017.1307733
5. O'Laughlin MP, Perry SB, Lock JE, Mullins CE (1991) Use of endovascular stents in congenital heart disease. Circulation 83(6):1923–1939
6. Boe BA, Zampi JD, Schumacher KR, Yu S, Armstrong AK (2016) The use and outcomes of small, medium and large premounted stents in pediatric and congenital heart disease. Pediatric Cardiol 37(8):1525–1533. https://doi.org/10.1007/s00246-016-1466-8
7. Eichhorn JG, Long FR, Hill SL, O'Donovan J, Chisolm JL, Fernandez SA, Cheatham JP (2006) Assessment of in-stent stenosis in small children with congenital heart disease using multi-detector computed tomography: a validation study. Catheter Cardiovasc Interv 68(1):11–20. https://doi.org/10.1002/ccd.20760
8. Ehara M, Kawai M, Surmely JF, Matsubara T, Terashima M, Tsuchikane E, Kinoshita Y, Ito T, Takeda Y, Nasu K, Tanaka N, Murata A, Fujita H, Sato K, Kodama A, Katoh O, Suzuki T (2007) Diagnostic accuracy of coronary in-stent restenosis using 64-slice computed tomography: comparison with invasive coronary angiography. J Am Coll Cardiol 49(9):951–959. https://doi.org/10.1016/j.jacc.2006.10.065

9. Gorenoi V, Schonermark MP, Hagen A (2012) CT coronary angiography vs. invasive coronary angiography in CHD. GMS Health Technol Assess 8:Doc02. https://doi.org/10.3205/hta000100
10. Eichhorn JG, Long FR, Jourdan C, Heverhagen JT, Hill SL, Raman SV, Cheatham JP (2008) Usefulness of multidetector CT imaging to assess vascular stents in children with congenital heart disease: an in vivo and in vitro study. Catheter Cardiovasc Interv 72(4):544–551. https://doi.org/10.1002/ccd.21680
11. Sun Z, Ng KH, Sarji SA (2010) Is utilisation of computed tomography justified in clinical practice? Part IV: applications of paediatric computed tomography. Singapore Med J 51(6):457–463
12. Brody AS, Frush DP, Huda W, Brent RL (2007) Radiation risk to children from computed tomography. Pediatrics 120(3):677–682. https://doi.org/10.1542/peds.2007-1910
13. Shah NB, Platt SL (2008) ALARA: is there a cause for alarm? Reducing radiation risks from computed tomography scanning in children. Curr Opin Pediatr 20(3):243–247. https://doi.org/10.1097/MOP.0b013e3282ffafd2
14. Mahnken AH (2012) CT imaging of coronary stents: past, present, and future. ISRN Cardiol 2012:139823. https://doi.org/10.5402/2012/139823
15. Petersilka M, Bruder H, Krauss B, Stierstorfer K, Flohr TG (2008) Technical principles of dual source CT. Eur J Radiol 68(3):362–368. https://doi.org/10.1016/j.ejrad.2008.08.013
16. Booij R, Dijkshoorn ML, van Straten M, du Plessis FA, Budde RP, Moelker A, Krestin GP, Ouhlous M (2016) Cardiovascular imaging in pediatric patients using dual source CT. J Cardiovasc Comput Tomogr 10(1):13–21. https://doi.org/10.1016/j.jcct.2015.10.003
17. Li T, Zhao S, Liu J, Yang L, Huang Z, Li J, Luo C, Li X (2017) Feasibility of high-pitch spiral dual-source CT angiography in children with complex congenital heart disease compared to retrospective-gated spiral acquisition. Clin Radiol 72(10):864–870. https://doi.org/10.1016/j.crad.2017.05.005
18. Nie P, Wang X, Cheng Z, Ji X, Duan Y, Chen J (2012) Accuracy, image quality and radiation dose comparison of high-pitch spiral and sequential acquisition on 128-slice dual-source CT angiography in children with congenital heart disease. Eur Radiol 22(10):2057–2066. https://doi.org/10.1007/s00330-012-2479-1
19. American Association of Physicists in Medicine (2008) The measure, reporting and management of radiation dose in CT. Report # 96 of AAPM task Group 23 of the Diagnostic Imaging Council CT Committee
20. Layritz C, Schmid J, Achenbach S, Ulzheimer S, Wuest W, May M, Ropers D, Klinghammer L, Daniel WG, Pflederer T, Lell M (2014) Accuracy of prospectively ECG-triggered very low-dose coronary dual-source CT angiography using iterative reconstruction for the detection of coronary artery stenosis: comparison with invasive catheterization. Eur Heart J Cardiovasc Imag 15(11):1238–1245. https://doi.org/10.1093/ehjci/jeu113
21. Rybicki FJ, Otero HJ, Steigner ML, Vorobiof G, Nallamshetty L, Mitsouras D, Ersoy H, Mather RT, Judy PF, Cai T, Coyner K, Schultz K, Whitmore AG, Di Carli MF (2008) Initial evaluation of coronary images from 320-detector row computed tomography. Int J Cardiovasc Imag 24(5):535–546. https://doi.org/10.1007/s10554-008-9308-2
22. Viera AJ, Garrett JM (2005) Understanding interobserver agreement: the kappa statistic. Fam Med 37(5):360–363
23. Nordmeyer J, Gaudin R, Tann OR, Lurz PC, Bonhoeffer P, Taylor AM, Muthurangu V (2010) MRI may be sufficient for noninvasive assessment of great vessel stents: an in vitro comparison of MRI, CT, and conventional angiography. Am J Roentgenol 195(4):865–871. https://doi.org/10.2214/ajr.09.4166
24. den Harder AM, Sucha D, van Hamersvelt RW, Budde RP, de Jong PA, Schilham AM, Bos C, Breur JM, Leiner T (2017) Imaging of pediatric great vessel stents: computed tomography or magnetic resonance imaging? PLoS One 12(1):e0171138. https://doi.org/10.1371/journal.pone.0171138
25. Achenbach S, Marwan M, Ropers D, Schepis T, Pflederer T, Anders K, Kuettner A, Daniel WG, Uder M, Lell MM (2010) Coronary computed tomography angiography with a consistent dose below 1 mSv using prospectively electrocardiogram-triggered high-pitch spiral acquisition. Eur Heart J 31(3):340–346. https://doi.org/10.1093/eurheartj/ehp470
26. Kanie Y, Sato S, Tada A, Kanazawa S (2017) Image Quality of coronary arteries on non-electrocardiography-gated High-Pitch Dual-Source computed tomography in children with congenital heart disease. Pediatric Cardiol. https://doi.org/10.1007/s00246-017-1675-9
27. Liu Y, Li J, Zhao H, Jia Y, Ren J, Xu J, Hao Y, Zheng M (2016) Image quality and radiation dose of dual-source CT cardiac angiography using prospective ECG-triggering technique in pediatric patients with congenital heart disease. J Cardiothorac Surg 11:47. https://doi.org/10.1186/s13019-016-0460-9
28. Zhao L, Zhang Z, Fan Z, Yang L, Du J (2011) Prospective versus retrospective ECG gating for dual source CT of the coronary stent: comparison of image quality, accuracy, and radiation dose. Eur J Radiol 77(3):436–442. https://doi.org/10.1016/j.ejrad.2009.09.006
29. Rengier F, Geisbusch P, Vosshenrich R, Muller-Eschner M, Karmonik C, Schoenhagen P, von Tengg-Kobligk H, Partovi S (2013) State-of-the-art aortic imaging: part I - fundamentals and perspectives of CT and MRI. VASA Zeitschrift fur Gefasskrankheiten 42(6):395–412. https://doi.org/10.1024/0301-1526/a000309
30. Rinaudo A, D'Ancona G, Baglini R, Amaducci A, Follis F, Pilato M, Pasta S (2015) Computational fluid dynamics simulation to evaluate aortic coarctation gradient with contrast-enhanced CT. Comput Methods Biomech Biomed Eng 18(10):1066–1071. https://doi.org/10.1080/10255842.2013.869321
31. Marrocco-Trischitta MM, van Bakel TM, Romarowski RM, de Beaufort HW, Conti M, van Herwaarden JA, Moll FL, Auricchio F, Trimarchi S (2018) The modified arch landing areas nomenclature (MALAN) improves prediction of stent graft displacement forces: proof of concept by computational fluid dynamics modelling. Eur J Vasc Endovasc Surg 55(4):584–592. https://doi.org/10.1016/j.ejvs.2017.12.019
32. Karmonik C, Muller-Eschner M, Partovi S, Geisbusch P, Ganten MK, Bismuth J, Davies MG, Bockler D, Loebe M, Lumsden AB, von Tengg-Kobligk H (2013) Computational fluid dynamics investigation of chronic aortic dissection hemodynamics versus normal aorta. Vasc Endovasc Surg 47(8):625–631. https://doi.org/10.1177/1538574413503561
33. Karmonik C, Partovi S, Davies MG, Bismuth J, Shah DJ, Bilecen D, Staub D, Noon GP, Loebe M, Bongartz G, Lumsden AB (2013) Integration of the computational fluid dynamics technique with MRI in aortic dissections. Magn Reson Med 69(5):1438–1442. https://doi.org/10.1002/mrm.24376
34. Pache G, Grohmann J, Bulla S, Arnold R, Stiller B, Schlensak C, Langer M, Blanke P (2011) Prospective electrocardiography-triggered CT angiography of the great thoracic vessels in infants and toddlers with congenital heart disease: feasibility and image quality. Eur J Radiol 80(3):e440–e445. https://doi.org/10.1016/j.ejrad.2011.01.032
35. Oberhoffer R, Lang D, Feilen K (1989) The diameter of coronary arteries in infants and children without heart disease. Eur J Pediatrics 148(5):389–392
36. Eichhorn JG, Jourdan C, Hill SL, Raman SV, Cheatham JP, Long FR (2008) CT of pediatric vascular stents used to treat congenital heart disease. Am J Roentgenol 190(5):1241–1246. https://doi.org/10.2214/ajr.07.3194
37. Eichhorn JG, Long FR, Hill SL, Cheatham JP (2006) Multislice computed tomography as an adjunct to the management of an

in-stent stenosis in an infant with congenital heart disease: imaging for the future. Catheter Cardiovasc Intervent 67(3):477–481. https://doi.org/10.1002/ccd.20644
38. Eisentopf J, Achenbach S, Ulzheimer S, Layritz C, Wuest W, May M, Lell M, Ropers D, Klinghammer L, Daniel WG, Pflederer T (2013) Low-dose dual-source CT angiography with iterative reconstruction for coronary artery stent evaluation. JACC Cardiovasc Imag 6(4):458–465. https://doi.org/10.1016/j.jcmg.2012.10.023
39. Husmann L, Leschka S, Desbiolles L, Schepis T, Gaemperli O, Seifert B, Cattin P, Frauenfelder T, Flohr TG, Marincek B, Kaufmann PA, Alkadhi H (2007) Coronary artery motion and cardiac phases: dependency on heart rate -- implications for CT image reconstruction. Radiology 245(2):567–576. https://doi.org/10.1148/radiol.2451061791
40. Mani G, Feldman MD, Patel D, Agrawal CM (2007) Coronary stents: a materials perspective. Biomaterials 28(9):1689–1710. https://doi.org/10.1016/j.biomaterials.2006.11.042
41. Jorge C, Dubois C (2015) Clinical utility of platinum chromium bare-metal stents in coronary heart disease. Med Devices (Auckland NZ) 8:359–367. https://doi.org/10.2147/mder.s69415
42. Hanawa T (2009) Materials for metallic stents. J Artif Organs 12(2):73–79. https://doi.org/10.1007/s10047-008-0456-x
43. Gwon DI, Ko GY, Kim JH, Shin JH, Yoon HK, Sung KB (2013) Malignant superior vena cava syndrome: a comparative cohort study of treatment with covered stents versus uncovered stents. Radiology 266(3):979–987. https://doi.org/10.1148/radiol.12120517
44. Kim SH, Choi YH, Cho H-H, Lee SM, Shin S-M, Cheon J-E, Kim WS, Kim I-O (2016) Comparison of image quality and radiation dose between high-Pitch Mode and Low-Pitch Mode Spiral chest CT in small uncooperative children: the effect of respiratory rate. Eur Radiol 26(4):1149–1158. https://doi.org/10.1007/s00330-015-3930-x
45. Lell MM, May M, Deak P, Alibek S, Kuefner M, Kuettner A, Kohler H, Achenbach S, Uder M, Radkow T (2011) High-pitch spiral computed tomography: effect on image quality and radiation dose in pediatric chest computed tomography. Invest Radiol 46(2):116–123. https://doi.org/10.1097/RLI.0b013e3181f33b1d
46. Guberina N, Lechel U, Forsting M, Ringelstein A (2016) Efficacy of high-pitch CT protocols for radiation dose reduction. J Radiol Prot 36(4):N57–Nn66. https://doi.org/10.1088/0952-4746/36/4/n57
47. Xia Y, Junjie Y, Ying Z, Bai H, Qi W, Qinhua J, Yundai C (2013) Accuracy of 128-slice dual-source CT using high-pitch spiral mode for the assessment of coronary stents: first in vivo experience. Eur J Radiol 82(4):617–622. https://doi.org/10.1016/j.ejrad.2012.11.033